Available online at www.sciencedirect.com

ScienceDirect

Ceramics International 40 (2014) 1807–1814

CERAMICS INTERNATIONAL

www.elsevier.com/locate/ceramint

Effect of the volume fraction of SiC on the microstructure and creep behavior of hot pressed Al_2O_3/SiC composites

M. Parchovianský[a,*], D. Galusek[b], M. Michálek[a], P. Švančárek[b], M. Kašiarová[c], J. Dusza[c], M. Hnatko[d]

[a]*Faculty of Chemical and Food Technology STU, Radlinského 9, 812 37 Bratislava, Slovakia*

[b]*Vitrum Laugaricio—Joint Glass Center of the Institute of Inorganic Chemistry, SAS, Alexander Dubček University of Trenčín, and RONA, j.s.c, Študentská 2, 911 50 Trenčín, Slovakia*

[c]*Institute of Materials Research, Slovak Academy of Sciences, Watsnova 47, SK-043 53 Košice, Slovakia*

[d]*Institute of Inorganic Chemistry, Slovak Academy of Sciences, Dúbravská cesta 9, SK-845 36 Bratislava, Slovakia*

Received 11 June 2013; received in revised form 8 July 2013; accepted 16 July 2013
Available online 24 July 2013

Abstract

Al_2O_3/SiC composites containing different volume fractions (3, 5, 10, 15, and 20 vol%) of SiC particles have been fabricated by mixing alumina and silicon carbide powders, followed by hot pressing at the temperature 1740 °C for 1 h under the pressure of 30 MPa and in the atmosphere of Ar. The effect of the volume fraction of SiC on the microstructure and creep behavior of the composites was investigated and possible creep mechanisms were discussed. The creep behavior of the composites at temperatures up to 1350 °C, and mechanical load up to 200 MPa, i.e. under conditions which were more severe than those reported previously, was studied, and compared to the monolithic Al_2O_3 reference. The microstructure and creep behavior of the Al_2O_3/SiC microcomposites was significantly influenced by the volume fraction of SiC particles and the average size of the alumina matrix grains. When compared to monolithic Al_2O_3, the creep resistance of the Al_2O_3/SiC composites was markedly improved, especially in the materials with 10 vol% of SiC. Long loading time before mechanical failure suggested grain boundary sliding and cavitation controlled creep behavior. The enhanced creep resistance was attributed to grain boundary pinning by the intergranular SiC nanoparticles.
© 2013 Elsevier Ltd and Techna Group S.r.l. All rights reserved.

Keywords: C. Creep; D. Al_2O_3/SiC; Microcomposites; Microstructure

1. Introduction

In the past few decades Al_2O_3/SiC nanocomposites have been widely studied, especially from the point of view of their mechanical properties. A number of authors figured out that the incorporation of a relatively small amount of SiC nanoinclusions into a Al_2O_3 matrix significantly enhanced the mechanical properties of alumina at room temperature, such as hardness [1,2], fracture toughness [3] and fracture strength [4–6]. The high temperature mechanical properties were also influenced. Niihara et al. [4] reported the improvement of the room temperature fracture strength to over 1 GPa in composites containing 5 vol% of SiC nanoparticles, as well as improvement of the high temperature mechanical properties. Other authors concluded that the addition of SiC into the Al_2O_3 matrix increased the creep resistance of the Al_2O_3/SiC nanocomposites by one to two orders of magnitude in comparison to monolithic Al_2O_3 [7,8]. The mechanisms responsible for the improvement of the creep resistance of Al_2O_3/SiC nanocomposites are still under investigation [9,10]. It has been proposed that the improvement of the creep resistance of Al_2O_3/SiC nanocomposites is caused by residual stresses, which are created in the Al_2O_3 matrix around SiC inclusions in the course of cooling from the temperature of sintering, as the result of the difference of thermal expansion coefficients of the matrix and the reinforcing particles. As suggested by Ohji et al. [11], the inherent stresses present at the alumina/SiC interfaces are compressive, which then results in stronger particle/matrix bonding, and thereby an improved

*Corresponding author. Tel.: +421 94 4600882.
E-mail address: parchoviansky@centrum.sk (M. Parchovianský).

0272-8842/$ - see front matter © 2013 Elsevier Ltd and Techna Group S.r.l. All rights reserved.
http://dx.doi.org/10.1016/j.ceramint.2013.07.081

creep resistance. Another mechanism in question is the grain boundary pinning by the intergranular SiC particles. The SiC particles rotate, and are engaged with the Al_2O_3 grains, thereby inhibiting the grain boundary sliding during the creep test, and reducing the strain rate of Al_2O_3/SiC nanocomposites [12]. Descamps et al. [13] also assume that the main factor controlling the high temperature strain of nanocomposites is the pinning of grain boundaries by SiC nanoparticles; as a consequence the grain boundary sliding is reduced. Ohji et al. [14] accomplished creep tests for both Al_2O_3/SiC nanocomposites with 17 vol% of SiC nanoparticles and monolithic Al_2O_3 at temperatures up to 1300 °C, and at mechanical loads ranging from 50 to 150 MPa. The creep resistance of the Al_2O_3/SiC composites was significantly higher when compared to the creep resistance of the monolithic Al_2O_3. The minimum creep rate of the Al_2O_3/SiC nanocomposite was about three orders of magnitude lower, and the creep life 10 times longer than that of the monolithic Al_2O_3 under the same mechanical load. The authors assume that the actual mechanism responsible for the remarkable improvement of the creep resistance of the Al_2O_3/SiC nanocomposites is strong interfacial bonding between Al_2O_3 and SiC, and inhibition of grain boundary diffusion by intergranular SiC particles. In other words, the Al_2O_3/SiC interface is much stronger than the alumina/alumina interface, the interfacial fracture energy of the Al_2O_3/SiC interface being two times higher than the interfacial fracture energy of the alumina/alumina boundary. The addition of 5 vol% of SiC to the Al_2O_3-based nanocomposites studied by Thompson et al. [15] led to the improvement of creep resistance similar to the results of Ohji [14], but the lower amount of SiC particles resulted in reduced number of intergranular creep cavities and much longer creep life. On the other hand, Deng et al. [16] observed an increase of the creep rate in the Al_2O_3-based nanocomposite containing 10 vol % of SiC particles. This was attributed to surface oxidation of the SiC particles, and the formation of an amorphous silica grain boundary film with subsequent decrease of the strength of the Al_2O_3/SiC interface bonding.

This work brings the first results of a study focused at the systematic investigation of creep behavior of alumina–silicon carbide composites, particularly the creep behavior at higher temperatures (1350 °C) and higher applied stresses (75–200 MPa) than usually used in majority of the studies on the creep behavior of this class of materials. The aim of this work was a detailed study of the relations between the microstructural parameters of Al_2O_3/SiC micro–nano-composites (grain size of the alumina matrix grains and distribution of the SiC particles) and their creep properties, a direct comparison of the effect of significantly different volume fractions of the SiC particles on the microstructure and creep behavior of the composites, and the determination of the optimum content of SiC. The paper summarizes the results on the creep behavior of the nanocomposites with different volume fractions of coarse grained (mean size 200 nm) SiC particles. The creep behavior of the composite materials is compared with the creep behavior of the monolithic alumina reference. Possible creep deformation controlling mechanisms are also discussed.

2. Experimental

Ultrafine high purity α-Al_2O_3 powder Taimicron TM-DAR (Taimei Chemicals Co., Ltd., Tokyo, Japan) and β-SiC powder (Superior Graphite Co., Ltd., Shanghai, China) were used as the starting materials. The characteristics of the starting powders are listed in Table 1 (data provided by the manufacturers). In order to investigate the effect of the different volume fractions of the SiC particles on the microstructure and the creep behavior of the Al_2O_3/SiC microcomposites, 3, 5, 10, 15, and 20 vol% of the SiC particles were added to Al_2O_3. The mixtures of Al_2O_3 and SiC powders were homogenized in a plastic jar on rollers in isopropyl alcohol for 24 h using high purity alumina balls. Thereafter, the mixtures were dried in a vacuum evaporator. The dried powders were crushed with a pestle in an agate mortar and sieved through a 100 μm mesh screen. The green bodies were prepared by uniaxial pressing from sieved powders in a graphite die with a maximum applied pressure of 30 MPa. Dense Al_2O_3/SiC microcomposites were fabricated by hot pressing in a rectangular graphite die (60×60 mm^2) for 1 h under 30 MPa uniaxial pressure and Ar protective atmosphere at 1740 °C. A BN layer was used as the high temperature protective bed. As a reference, monolithic Al_2O_3 ceramics was prepared under the same experimental conditions (i.e. homogenization, drying, sieving, and consolidation). The green body was hot pressed at a temperature of 1350 °C under a pressure of 30 MPa for 1 h in vacuum, using the BN protective bed. The sintering temperature was reduced to 1350 °C in order to prepare the monolithic Al_2O_3 with the mean size of matrix grain comparable to that in the Al_2O_3/SiC composites.

The bulk densities of the composite samples were measured by the Archimedes method in mercury. The relative densities were obtained as the ratio of the Archimedes densities and the physical densities calculated by the rule of mixtures, using the physical densities of α-Al_2O_3 and β-SiC (3.98 and 3.21 g/cm^3, respectively). The microstructure of prepared composites was examined on polished and thermally etched cross sections by scanning electron microscopy (JEOL JSM 7600F). Thermal etching of the composites was carried out in a graphite furnace at a temperature of 1350 °C for 1 h in the atmosphere of Ar in order to delineate grain boundaries. The average grain size was determined by the linear intercept method (program Lince, TU Darmstadt, Germany). A minimum of 200 grains was measured in order to obtain statistically sufficiently large set of data. The dense materials were cut into rectangular bars with the size of $4 \times 3 \times 45$ mm and ground flat using an automatic grinding machine JUNG JE525. Prior to creep testing the

Table 1
Basic characteristics of the starting powders as provided by the producers.

Powder	Density [g/cm^3]	Specific surface area [g/m^2]	Average particle size [nm]	Purity [%]
α-Al_2O_3	3.98	14.5	170	99.995
β-SiC	3.21	13.5–18.5	200	97–99

tensile faces of all test bars were ground to a 15 μm surface finish with a diamond grinding wheel, and the edges were chamfered to eliminate defects introduced by machining. The creep tests were carried out in a four-point bending mode (20/40 inner/outer span) at the temperature 1350 °C, under applied stresses ranging from 75 to 200 MPa in the inert atmosphere of argon. In addition, creep tests were also accomplished at the temperatures 1400 °C and 1450 °C for the AS10 composite sample, also under applied stresses ranging from 75 to 200 MPa in the inert atmosphere of argon. The sample deflection was recorded continuously during the creep test. In order to determine the stress exponent n the applied stress was gradually changed during the test. Stationary creep rates were first calculated from the height of the creep rate steps obtained from the stress change tests. The values of the stationary creep rates were plotted as a function of the applied stress, and the stress exponent n was determined as the slope of the curve.

Table 2
Basic characteristics of the studied materials.

Samples	SiC content [vol%]	Relative density [%]	Average size of the Al_2O_3 matrix grains [μm]
A	0	98.3	1.4 ± 0.4
AS3	3	99.6	14.2 ± 1.1
AS5	5	99.4	10.9 ± 0.2
AS10	10	99.4	1.8 ± 0.2
AS15	15	99.4	1.1 ± 0.2
AS20	20	99.3	0.6 ± 0.1

3. Results and discussion

3.1. Microstructure before creep

The basic characteristics of all prepared materials are summarized in Table 2. The mean size of the Al_2O_3 matrix grains in the composites decreased with increasing SiC content. The microstructure of the monolithic Al_2O_3 reference (Fig. 1a)

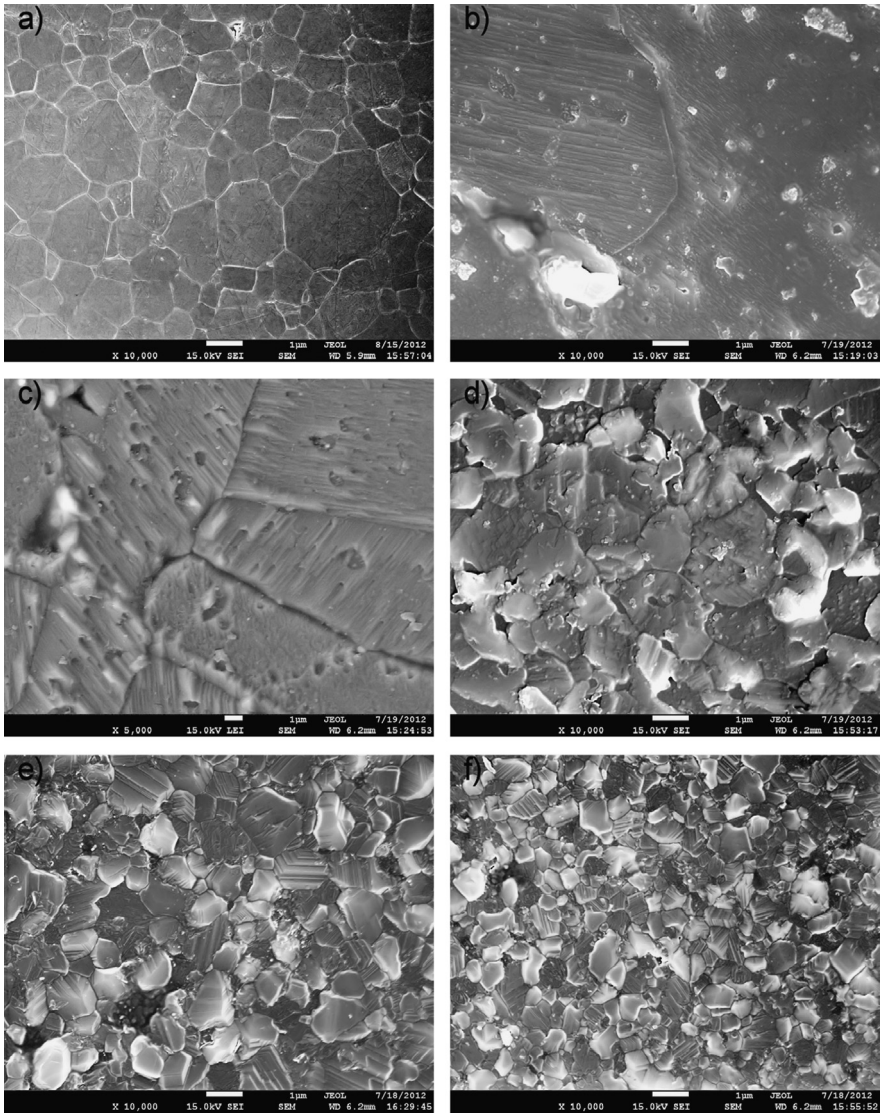

Fig. 1. Microstructures of monolithic Al_2O_3 and Al_2O_3/SiC nanocomposites prior to the creep tests: (a) Al_2O_3, (b) AS3, (c) AS5, (d) AS10, (e) AS15, and (f) AS20.

was relatively finer than the microstructure of the composites AS3 (Fig. 1b) and AS5 (Fig. 1c). The mean grain size was only 1.5 μm, due to lower sintering temperature (1350 °C) applied for densification of the monolithic alumina reference. The temperature of hot pressing of the composites was determined on the basis of the thermodynamic analysis of the system published in our previous work [17]. We demonstrated there SiO_2 as an impurity, which is always present at the surface of SiC particles, enters the reactions, which may result in complete disappearance of SiC at temperatures exceeding 1750 °C. This applies particularly in the absence of a protective powder bed that produces gaseous species (such as CO and SiO), which shift the reaction equilibrium towards the reactants. The results of the analysis were supported by the experimental data. The maximum temperature used in this work for the densification of the composites therefore did not exceed 1740 °C. The microstructure of the Al_2O_3/SiC composites was significantly influenced by the volume fraction of SiC particles. The growth of Al_2O_3 matrix grains was observed especially in the composites containing 3 (Fig. 1a) and 5 vol% (Fig. 1b) of SiC due to less efficient grain boundary pinning by a smaller number of intergranular SiC particles. As the amount of the SiC increased (10, 15, and 20 vol%), the microstructure (Fig. 1d–f) of the composites was significantly refined. The grain boundary mobility, and hence also the grain growth, were influenced by the volume fraction of SiC. The increasing number of intergranular SiC particles hindered the growth of alumina matrix grains by efficient grain boundary pinning. The microstructure of the nanocomposites with 20 vol% (Fig. 1f) of SiC particles was much finer than the microstructure of the nanocomposites sintered under the same condition, but containing less SiC. The retarding action of the SiC particles with respect to the grain boundary motion (i.e. the grain growth) is in general determined by their relative frequency with respect to the number of occupied sites at the grain boundary junctions, and by their size. The observed differences in the mean grain size were therefore the consequence of the different number, and volume, of the intergranular SiC particles: higher volume fraction of the SiC particles increased the total area of the SiC–alumina grain boundaries on account of the alumina–alumina boundaries, altering the energy requirements for grain boundary diffusion and grain boundary mobility. The grain boundaries tended to be pinned more efficiently by larger SiC particles, which were dragged along as the grain boundaries moved. Smaller SiC particles were generally less effective as the pinning sites; they were easily engulfed by the fast moving grain boundaries and tended to finish at intragranular positions.

3.2. Creep behavior

The high temperature creep rate $\dot{\varepsilon}$ of polycrystalline materials can be described by [18,19]

$$\dot{\varepsilon} = A\frac{DGb}{kT}\left(\frac{b}{d}\right)^{p}\left(\frac{\sigma}{G}\right)^{n} \quad (1)$$

where D is the appropriate diffusion coefficient, G is the shear modulus, b is Burger's vector, k is the Boltzmann constant, T is the absolute temperature, d is the grain size, p is the exponent of the inverse grain size, n is the stress exponent, and A is a dimensionless constant.

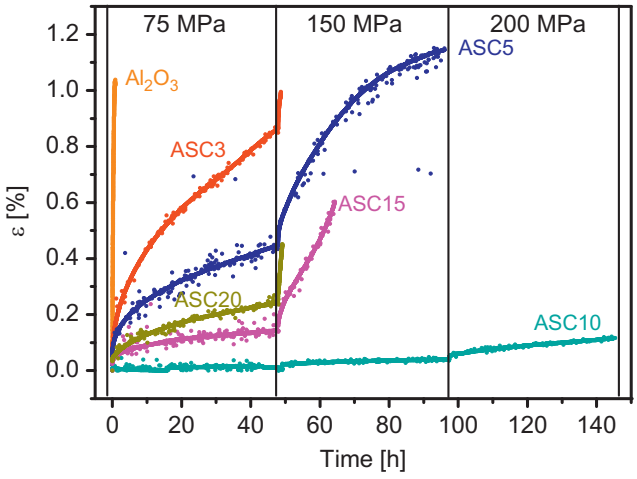

Fig. 2. Creep curves (strain–time plots) of the monolithic Al_2O_3 and of the Al_2O_3/SiC composites obtained at 1350 °C, under the applied stress ranging from 75 to 200 MPa.

It follows from Eq. (1) that each creep mechanism is uniquely specified by the values of the three constants, A, p and n, and by the activation energy, Q. In general, however, the experimental values of A depend rather critically on the precise values of p, n and Q, so that the dimensionless constant A is usually of little value in determining the precise deformation mechanisms. There exist several models for creep deformation. The main creep deformation mechanisms can be grouped into lattice mechanisms (dislocation glide, dislocation creep—Nabarro–Herring creep), and boundary mechanisms (diffusion creep—Coble creep, grain boundary sliding). Dislocation glide involves dislocations moving along slip planes and overcoming barriers by thermal activation, and occurs at high stress. The dislocation creep therefore includes dislocation movement to overcome barriers by diffusion of vacancies or interstitials. In the case of diffusion creep the flow of vacancies and interstitials through a crystal is influenced by the applied stress. Grain boundary sliding is associated with the sliding of grains past each other. Boundary mechanisms rely on the presence of grain boundaries and occur only in polycrystalline materials. They are associated with some dependence on grain size so that the parameter p assumes the values ≥1. On the other hand, the lattice mechanisms affect the interior of the grains, independently of their size, and the parameter p is therefore equal to zero. The values of the stress exponent n also depend on the mechanism that controls the creep deformation. For lattice diffusion (Nabarro–Herring creep) the value $n=1$, for surface diffusion (Coble creep) the stress exponent $n=2$, and for dislocation mechanisms it ranges from 3 to 5 [18,19].

Fig. 2 shows the creep curves (strain–time plots) of the monolithic Al_2O_3 reference, and of the Al_2O_3/SiC composites obtained under a step-wise regime (with a gradual increase of the applied stress from 75 to 200 MPa), and at a temperature of 1350 °C. The creep behavior of both the monolithic Al_2O_3 and

the nanocomposites was characterized by a short period of primary creep followed by a prolonged period of the steady-state creep, where the strain rate decreased with time. Tertiary creep was not observed. The creep resistance of all materials containing SiC particles was significantly higher when compared to the creep resistance of the monolithic Al_2O_3. If we compared the creep resistance of the Al_2O_3/SiC composites with various volume fractions of the SiC particles, Fig. 2, it was obvious that the creep resistance of the composites increased when the volume fraction of SiC is increased from 3 to 10 vol%. However, too high a SiC content (15 and 20 vol%) impaired the creep resistance. Particularly, the composite AS10 showed excellent creep resistance. From the creep curve it can be seen that the composite AS10 can withstand long lasting loading corresponding to a stress of 200 MPa at the temperature 1350 °C. At the same temperature the monolithic Al_2O_3 reference and other composite materials failed after being loaded to 75 MPa and 150 MPa, respectively. Even after 150 h of the creep test at 1350 °C and an applied stress of 200 MPa creep failure did not occur in the AS10 composite. This result suggested extremely high creep resistance of the material; creep tests at the temperatures 1400 and 1450 °C and under applied stresses ranging from 75 to 200 MPa were therefore also carried out. The results of the creep tests (strain–time plot) of the composite material AS10 are illustrated in Fig. 3. The creep deformation increased with the test temperature and applied stress. The composite AS10 failed at 1450 °C when the stress of 200 MPa was applied. The stress exponent n for the composite AS10 was determined as the slope of the linear fit of the dependence $\log \dot{\varepsilon}$ versus $\log \sigma$ (Fig. 4). The linear fit indicated that the stress exponents n of the composite AS10 assumed relatively high, and similar, values of $n=3.4$ and 3.5 at 1350 °C and 1400 °C, respectively, while the stress exponent at 1450 °C assumed a lower value $n=2.6$. The stress exponents for the monolithic Al_2O_3 reference and the other composite materials could not be determined due to premature specimen failure at 75 MPa and 150 MPa, respectively. High values of the stress exponents of the composites are a common feature in materials where the creep-controlling mechanisms involve dislocation motion ($n=3$ or 5). The actual values then depend on whether the deformation process was controlled by dislocation glide or dislocation climb. Potential mechanisms, which control the high temperature deformation of the Al_2O_3/SiC nanocomposites, include also diffusion along grain boundaries or through the crystal lattice of the crystalline phases present. Jaafar et al. [20] conducted creep tests on Al_2O_3 based nanocomposites with 5 vol% of SiC particles and reported stress exponents of 4.7 and 4.2 at 1200 °C. They concluded that the creep rate controlling mechanism was dislocation motion. However, creep deformation mechanisms cannot be reliably inferred from the stress exponent values for multiphase materials and composite materials in particular. The stress exponent values determined at high stress levels ($n=2.6$–3.5) in this work were similar to the values reported by Jaafar et al. [20]. Grain-boundary sliding accompanied by boundary diffusion has been suggested to be the predominant deformation mechanism of monolithic Al_2O_3 at temperatures below 1400 °C [21]. We could therefore expect this to be the case also in the present work. The microstructures of the monolithic Al_2O_3 before and after the creep tests are illustrated in Figs. 1a and 5a, respectively. The SEM micrograph (Fig. 1a) shows the microstructure of the monolithic Al_2O_3 ceramic with monomodal grain size distribution and regular equiaxed grains. No obvious voids (cavities) or cracks could be detected. The microstructure examination of the monolithic Al_2O_3 after the creep test (Fig. 5a) revealed elongated grains with irregular grain boundaries, which suggested grain boundary sliding as the main deformation mechanism. The creep deformation mechanisms in the Al_2O_3/SiC nanocomposites could be expected to be similar, to certain extent, to those in the monolithic Al_2O_3 because grain boundary sliding is one of the principal creep mechanisms of all ceramic materials. However, some results [22,23] pointed to the existence of two stress-dependent deformation mechanisms. At low stress, grain boundary sliding controlled the deformation, while at high stress the creep deformation was controlled by creep

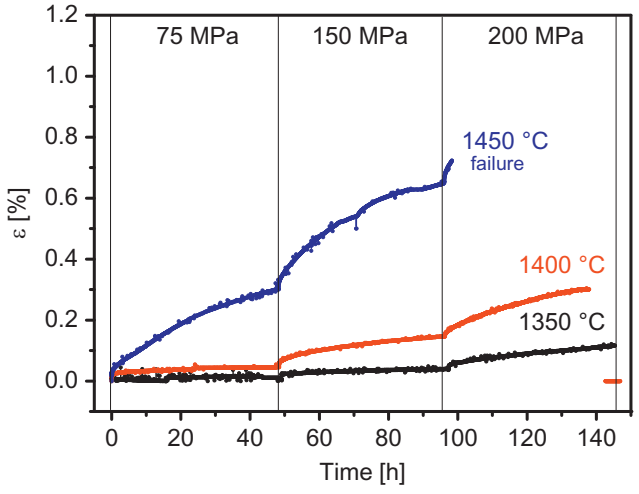

Fig. 3. Creep curves (strain–time plots) of the composite AS10 measured at 1350 °C, 1400 °C, and 1450 °C, under the applied stress ranging from 75 to 200 MPa.

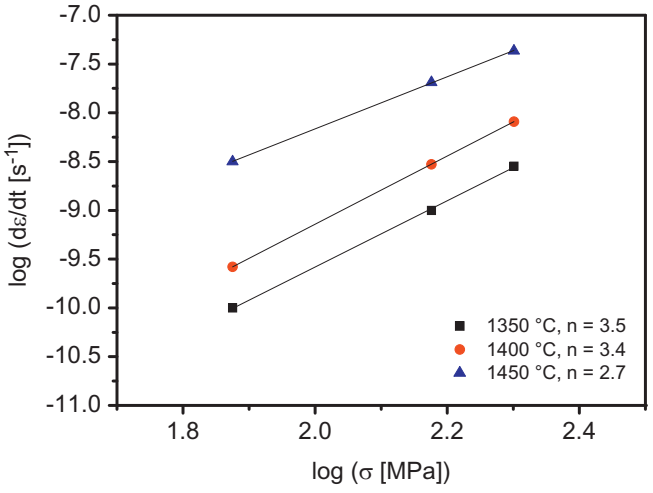

Fig. 4. Steady-state creep rate versus stress plot of the AS10 composite measured in the temperature range between 1350 °C and 1450 °C, under applied stresses from 75 to 200 MPa.

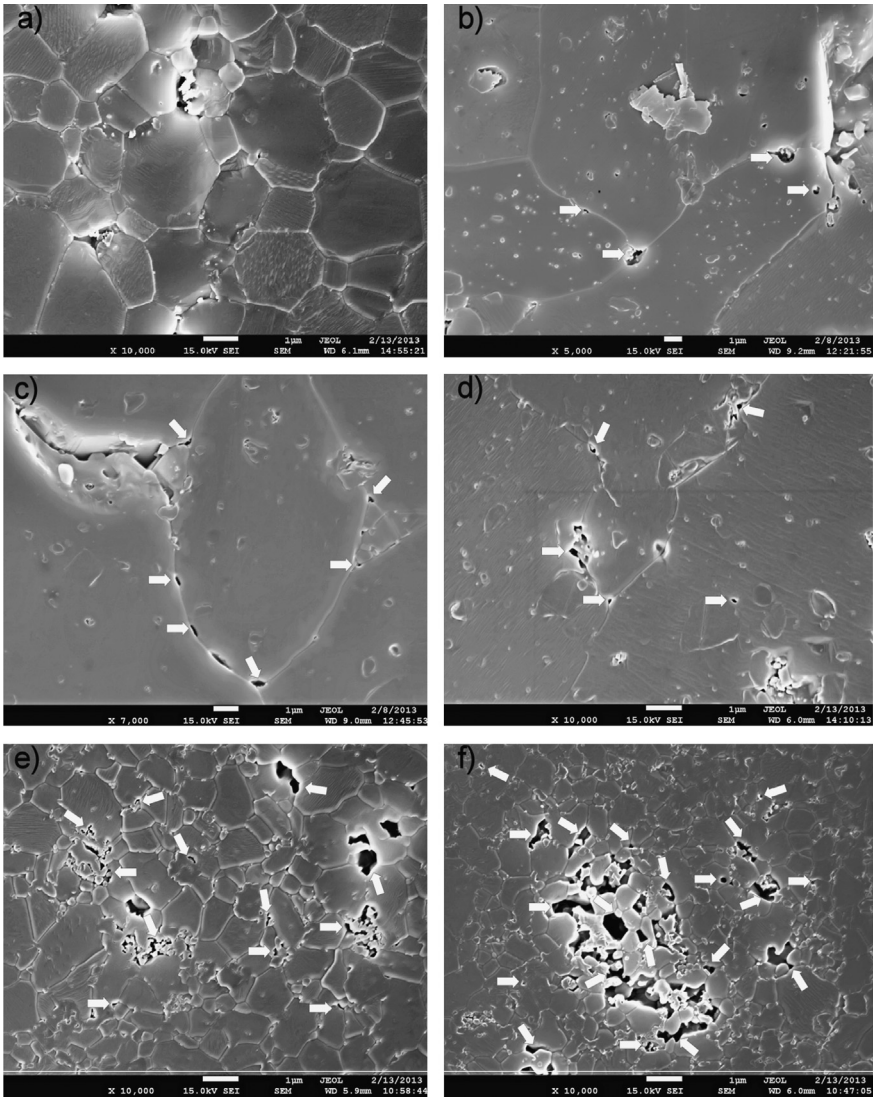

Fig. 5. Microstructures of monolithic Al_2O_3 and Al_2O_3/SiC nanocomposites after creep tests obtained at 1350 °C, under applied stresses ranging from 75 to 200 MPa; cavities at grain boundaries and in the triple grain boundary junctions are marked with white arrows. (a) Al_2O_3, (b) AS3, (c) AS5, (d) AS10, (e) AS15, and (f) AS20.

cavitation and microcracking caused by stress concentration. Ohji et al. [14] observed SiC particles at the grain boundaries which appeared rotating under the influence of grain boundary shear and creating cavities in the process. It could be therefore expected that the mechanisms of creep in the Al_2O_3/SiC nanocomposites studied in this work represented a complex form of interface controlled diffusion-assisted creep accompanied by grain boundary sliding and cavitation. SEM micrographs of the composite samples after the creep tests are shown in Fig. 5a–f. The microstructure examination (Fig. 5b and c) of the composite samples with lower volume fraction of SiC particles (3 and 5 vol %) after the creep test revealed few cavities at grain boundaries and in the triple grain boundary junctions. The microstructural features detected in the composites with higher volume fractions of SiC were different. The SEM micrographs in Fig. 5d–f revealed that the increasing volume fraction of SiC from 10 to 20 vol% led to extensive formation of intergranular voids and cavities. Grain boundary separation was also observed in some cases (Fig. 6a and b). In fact, cavity nucleation seemed to be associated both with the intergranular SiC particles and with the Al_2O_3/Al_2O_3 interfaces. In this case, cavities could be formed due to rotation of the SiC particles, which impeded grain boundary sliding under the influence of grain-boundary shear. While inhibiting grain boundary sliding, the grain boundary particles would also concentrate stress within the composite. The microstructure observations thus seemed to support the hypothesis that at higher temperatures and stresses the creep deformation was controlled mainly by grain boundary sliding and cavitation. This hypothesis is also in accord with the results of Niihara et al. who concluded that the inhibition of grain boundary sliding by SiC particles located at the matrix grain boundaries was responsible for improvement of the creep resistance of composite materials. However, for the Al_2O_3/SiC nanocomposites this hypothesis was only supported by Ohji et al. [14] who carried out the creep tests of both the Al_2O_3/SiC nanocomposites containing 17 vol% of SiC, and of the monolithic Al_2O_3 at temperatures up to 1300 °C,

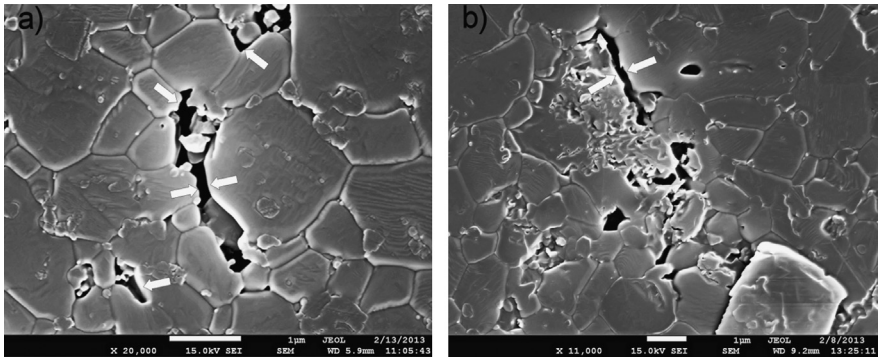

Fig. 6. Microstructures of Al_2O_3/SiC nanocomposites after creep tests obtained at 1350 °C, under applied stresses ranging from 75 to 200 MPa; grain boundary separations are marked with white arrows. (a) AS15 and (b) AS20.

and at applied stresses ranging from 50 to 150 MPa. They found the creep resistance of the Al_2O_3/SiC composites to be significantly higher. The minimum creep rate of the Al_2O_3/SiC nanocomposite was about three orders of magnitude lower and the creep life ten times longer than that of the monolithic Al_2O_3. The authors [14] assume that the actual mechanism responsible for the remarkable improvement of the creep resistance of the Al_2O_3/SiC nanocomposites was strong interface bonding between Al_2O_3 and SiC. As the consequence, the intergranular SiC particles inhibited grain boundary diffusion. However, the results obtained in this work indicated that high volume fraction of SiC impaired the creep resistance of the Al_2O_3-based composites. Descamps et al. [13] concluded that the creep resistance of Al_2O_3/SiC composites strongly depended on the mean size of alumina matrix grains, with the creep resistance of nanocomposites decreasing as the microstructure was refined. These findings were consistent with those obtained in this work: the increase of the volume fraction of SiC resulted in significant microstructure refinement. This seemed to be one of the reasons for the different creep behavior of the Al_2O_3/SiC nanocomposites in this study; the creep resistance was influenced by two competing parameters: the increasing volume fraction of the SiC particles on the one hand and the average size of alumina matrix grains on the other. The increase of the volume fraction of SiC from 3 to 10 vol% was beneficial, because it inhibited grain boundary sliding and enhanced grain boundary strength. The SiC particles located at the grain boundaries would also impede the motion of grain boundary dislocations that was often associated with grain-boundary sliding. On the other hand, a higher amount of SiC particles inhibited the growth of the Al_2O_3 matrix grains more effectively, resulting in increasing number of the grain boundaries, which could slide along each other. In this way deformation was supported and the creep resistance impaired. In other words, with the increasing content of SiC particles the mean size of the alumina matrix grains became smaller. According to Eq. (1) the steady-state creep rate depends on the grain size or, more specifically, on the term $1/d^p$ where d is the grain size and p the grain size exponent. It means that for the creep resistance the incorporation of lower volume fraction (3–10%) of SiC particles which leads to coarser microstructure was more beneficial in terms of improvement of the creep resistance. On the other hand, the addition of a higher amount of SiC particles (15–20 vol% of SiC) led to finer microstructure, even if the number of SiC particles at intergranular position was higher, and the creep resistance was lower. All these observations confirmed that the addition of SiC particles alone is not sufficient for obtaining composite materials with high creep resistance. The possible impact of the volume fraction, microstructure and the mean size of the alumina matrix grains must be also considered.

4. Conclusions

Al_2O_3/SiC composites containing different volume fractions (3, 5, 10, 15, and 20 vol%) of SiC were prepared by mixing alumina and silicon carbide powders, followed by hot pressing at 1740 °C. The influence of the volume fraction of SiC particles with a mean size of 200 nm on the microstructure and creep behavior of the composites was studied at temperatures up to 1450 °C, and mechanical loads up to 200 MPa. The results were compared to the creep behavior of a monolithic Al_2O_3 reference material. The microstructure of the Al_2O_3/SiC composites was significantly influenced by the addition, and volume fraction, of SiC. With the increasing amount of SiC the microstructure was refined. The creep resistance of the Al_2O_3/SiC composites was improved when compared to the creep resistance of the monolithic Al_2O_3. Particularly, the Al_2O_3/SiC composite with 10 vol% of SiC (material AS10) exhibited excellent creep resistance. The material was able to withstand stresses of 200 MPa at 1350 °C and 1400 °C for 150 h, while the monolithic Al_2O_3 failed already after 0.8 h at 1350 °C, and loads as low as 75 MPa. The creep resistance of the composites increased with increasing volume fraction of SiC in the concentration range between 3 and 10 vol%. However, too high a content of SiC (15 and 20 vol%) impaired the creep resistance significantly. The improvement of the creep resistance was attributed to the pinning effect of the SiC particles located at the grain boundaries. These inhibited grain boundary sliding and reduced the creep strain rate. However, in the composites the creep resistance decreased due to refinement of the matrix microstructure. The results confirmed that the addition of SiC particles alone was not sufficient for achieving highly creep resistant composite materials. Additional factors such as the volume fraction of SiC, microstructure, and the

mean size of the alumina matrix grains have to be also considered.

Acknowledgments

The financial support of this work by the APVV Grant LPP 0297-09, VEGA 1/0206/11, and the SAS-NSC-2010-02 Joint Research bilateral Project is gratefully acknowledged. This publication was created in the frame of the project "Centre of excellence for ceramics, glass, and silicate materials" ITMS code 262 201 20056, based on the Operational Program Research and Development funded from the European Regional Development Fund.

References

[1] X.L. Shi, F.M. Xu, Z.J. Zhang, Y.L. Dong, Y. Tan, L. Wang, M.J. Yang, Mechanical properties of hot pressed Al_2O_3/SiC composites, Materials Science and Engineering A 527 (2010) 4646–4649.

[2] Y.L. Dong, F.M. Xu, X.L. Shi, C. Zhang, Z.J. Zhang, J.M. Yang, Y. Tan, Fabrication and mechanical properties of nano-/micro-sized Al_2O_3/SiC composites, Materials Science and Engineering A 504 (2009) 49–54.

[3] Y. Xu, A. Zangvil, A. Kerber, SiC nanoparticle-reinforced Al_2O_3 matrix composites: role of intra- and intergranular particles, Journal of the European Ceramic Society 17 (1997) 921–928.

[4] K. Niihara, New design concept of structural ceramics—ceramic nanocomposites, Journal of the Ceramic Society of Japan 99 (1991) 974–982.

[5] L. Gao, J.S. Hong, H. Miyamoto, S.D.D.L. Torre, Bending strength and microstructure of Al_2O_3 ceramics densifed by spark plasma sintering, Journal of the European Ceramic Society 20 (2000) 2149–2152.

[6] M. Parchovianský, D. Galusek, J. Sedláček, P. Švančárek, M. Kašiarová, J. Dusza, P. Šajgalík, Microstructure and mechanical properties of hot pressed Al_2O_3/SiC nanocomposites, Journal of the European Ceramic Society 33 (2013) 2291–2298.

[7] Z.Y. Deng, J.L. Shi, Y.F. Zhang, T.R. Lai, J.K. Guo, Creep and creep behaviour in silicon carbide particle reinforced alumina, Journal of the American Ceramic Society 82 (1999) 944–952.

[8] H. Reveron, O. Zaafrani, G. Fantozzi, Microstructure development, hardness, toughness and creep behavior of pressureless sintered alumina/SiC micro/nano-composites obtained by slip-casting, Journal of the European Ceramic Society 30 (2010) 1351–1357.

[9] Q. Tai, A. Mocellin, Review: high temperature deformation of Al_2O_3-based ceramic particle or whisker composite, Ceramics International 25 (1999) 395–408.

[10] M. Sternitzke, Review: structural ceramic nanocomposites, Journal of the European Ceramic Society 17 (1997) 1061–1082.

[11] T. Ohji, T. Hirano, A. Nakahira, K. Niihara, Particle/matrix interface and its role in creep inhibition in alumina/silicon carbide nanocomposites, Journal of the American Ceramic Society 79 (1996) 33–45.

[12] Z.Y. Deng, Y.F. Zhang, J.L. Shi, J.K. Guo, D.Y. Jiang, Pinning effect of SiC particles on mechanical properties of Al_2O_3/SiC ceramic matrix composites, Journal of the European Ceramic Society 18 (1998) 501–508.

[13] P. Descamps, D. O'Sullivan, M. Poorteman, J.C. Descamps, A. Leriche, Creep behavior of Al_2O_3–SiC nanocomposites, Journal of the European Ceramic Society 19 (1999) 2475–2485.

[14] T. Ohji, A. Nakahira, T. Hirano, K. Niihara, Tensile creep behaviour of alumina/silicon carbide nanocomposite, Journal of the American Ceramic Society 77 (1994) 3259–3262.

[15] A.M. Thompson, H.M. Chan, M.P. Harmer, Tensile creep of alumina–silicon carbide nanocomposites, Journal of the American Ceramic Society 80 (1997) 2221–2228.

[16] Z.Y. Deng, Y.F. Zhang, J.L. Shi, J.K. Guo, Microstructure and flexure creep behavior of SiC particle reinforced Al_2O_3 matrix composites, Journal of the European Ceramic Society 16 (1996) 1337–1343.

[17] D. Galusek, R. Klement, J. Sedláček, M. Balog, C. Fasel, J. Zhang, M. A. Crimp, R. Riedel, Al_2O_3–SiC composites prepared by infiltration of pre-sintered alumina with a poly(allyl)carbosilane, Journal of the European Ceramic Society 31 (2011) 111–119.

[18] W.R. Cannon, T.G. Landon, Review creep of ceramics. Part 1 mechanical characteristics, Journal of Materials Science 18 (1983) 1–50.

[19] W.R. Cannon, T.G. Landon, Review creep of ceramics. Part 2 an examination of flow mechanism, Journal of Materials Science 23 (1988) 1–20.

[20] M. Jaafar, H. Reveron, C. Esnouf, G. Fantozzi, Highly creep-resistant alumina–SiC nanocomposites processed by spark plasma sintering, Scripta Materialia 68 (2013) 134–137.

[21] A.G. Robertson, D.S. Wilkinson, C.H. Caceres, Creep and creep fracture in hot pressed alumina, Journal of the American Ceramic Society 74 (1991) 922–933.

[22] P. Lipetzky, S.R. Nutt, P.F. Becher, Creep behaviour of an Al_2O_3–SiC composite, Materials Research Society Symposia Proceedings 120 (1988) 271–277.

[23] H.T. Lin, P.F. Becher, Creep behaviour of SiC whiskers reinforced alumina, Journal of the American Ceramic Society 120 (1999) 265–270.